

Probabilistic seismic evaluation of buckling restrained braced frames using DCFD and PSDA methods

Behrouz Asgarian^{1a}, Edris Salehi Golsefidi^{*2} and Hamed Rahman Shokrgozar^{3b}

¹Civil Engineering Faculty, K. N. Toosi University of Technology, Tehran, Iran

²Babol Noshirvani University of Technology, Mazandaran, Iran

³Faculty of Technical and Engineering, University of Mohaghegh Ardabili, Ardabil, Iran

(Received October 27, 2013, Revised April 11, 2015, Accepted November 16, 2015)

Abstract. In this paper, using the probabilistic methods, the seismic demand of buckling restrained braced frames subjected to earthquake was evaluated. In this regards, 4, 6, 8, 10, 12 and 14-story buildings with different buckling restrained brace configuration (including diagonal, split X, chevron V and Inverted V bracings) were designed. Because of the inherent uncertainties in the earthquake records, incremental dynamical analysis was used to evaluate seismic performance of the structures. Using the results of incremental dynamical analysis, the “capacity of a structure in terms of first mode spectral acceleration”, “fragility curve” and “mean annual frequency of exceeding a limit state” was determined. “Mean annual frequency of exceeding a limit state” has been estimated for immediate occupancy (IO) and collapse prevention (CP) limit states using both Probabilistic Seismic Demand Analysis (PSDA) and solution “based on displacement” in the Demand and Capacity Factor Design (DCFD) form. Based on analysis results, the inverted chevron (Λ) buckling restrained braced frame has the largest capacity among the considered buckling restrained braces. Moreover, it has the best performance among the considered buckling restrained braces. Also, from fragility curves, it was observed that the fragility probability has increased with the height.

Keywords: buckling restrained braced frame; performance-based earthquake engineering; incremental dynamic analysis; fragility curve; mean annual frequency

1. Introduction

Damage to steel structures during 1994 Northridge and 1995 Kobe earthquakes illustrated the need to do more research in order to improve performance of steel structures subjected to strong ground motion. Changes to steel braced frame system have led to do more research and development of buckling restrained braced frames to improve behavior of braced frames in nonlinear range of deformation. After serious damages to building with ordinary braced frames in 1994 Northridge and 1995 Kobe earthquakes (Rai and Goel 2003), the use of this structural system

*Corresponding author, Ph.D. Student, E-mail: es.golsefidi@gmail.com

^aAssociate Professor, E-mail: asgarian@kntu.ac.ir

^bAssistant Professor, E-mail: h_rshokrgozar@uma.ac.ir

with high slenderness ratio has been avoided due to their low ductility, low energy absorption and rapid strength and stiffness degradation during strong ground motion.

The buckling restrained braces yield in both tension and compression and has stable hysteresis curve during cyclic inelastic large deformation. In this type of bracing system, by increasing the compression strength via postponing Buckling modes, the compression and tension capacities get almost equal and one gets almost symmetric behavior in both tension and compression of hysteresis curves. (Kumar *et al.* 2007) It has been depicted in Fig. 1. (Clark *et al.* 1999) The buckling restrained braced frames consist of a ductile steel core which yields in compression and tension. It has also a mechanism to prevent buckling which usually consists of steel casing and mortar. An unbonding material or a very small air gap to minimize transferring axial force from the core to the buckling resistant mechanism is another component of this type of bracing. (Bozorgnia *et al.* 2003)

Young *et al.* (2009) conducted a study to investigate effect of design parameters such as constraining tube thickness, unconstrained length of core ends on maximum strength and energy dissipation capability of buckling restrained braces. In accordance with it, the thickness of the external tube and the unconstrained part of the core had a significant effect on the strength and hysteretic behavior of the BRB. Asgarian and Shokrgozar (2009) determined the seismic response modification factor of BRBF by using incremental dynamic analysis and pushover analysis. Lin *et al.* (2009) calculated the seismic reliability of buckling restrained frames, eccentrically braced frames and moment resisting frames in both near field and far field cases. Güneysi (2011), determined the seismic reliability of retrofitted moment resisting frames using buckling restrained braced frames. Hoveidaea *et al.* (2012) studied overall buckling behavior of all steel buckling restrained braces. Park *et al.* (2012) carried out cyclic test of buckling restrained braces composed of square steel rods and steel tube. Eventually, the test result showed BRBs with continuous steel rods as filler material had good performance when the external tubes were strong enough against buckling.

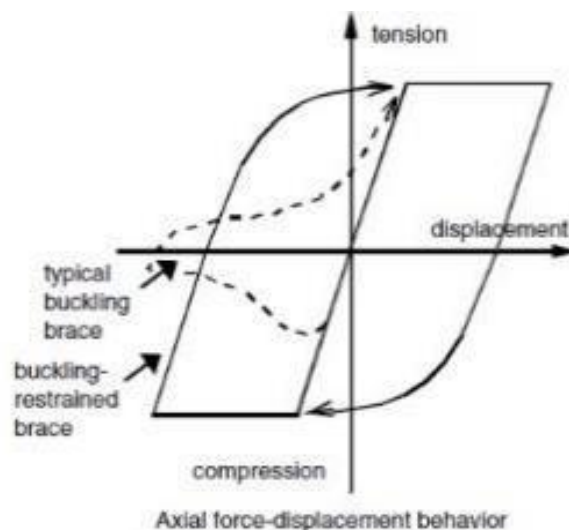


Fig. 1 Difference in energy dissipation between conventional brace and BRB under cyclic loading a) conventional brace b) BRB (Clark *et al.* 1999)

In this paper, incremental dynamic analysis is used to compute probabilistic parameters such as hazard drift and mean annual frequency of exceeding limit states. In this kind of analysis capacity and limit states of a structure are estimated using a set of nonlinear dynamic analysis. Based on this, chosen ground motions are rescaled in each step to cover whole of structure behavior from linear elastic behavior to global collapse. Using statistical methods and appropriate parameters for seismic hazard analysis, the capacity of the structure, fragility curves and mean annual frequency are calculated.

2. Probabilistic seismic demand analysis (PSDA) and solving strategy based on displacement in the form of Demand-Capacity Factor Design (DCDF)

Probabilistic seismic demand analysis combines seismic hazard analysis of a specific site with demand results from nonlinear dynamic analysis. Mean annual frequency of exceeding a limit state is defined as the product of the average rate of occurrence of a certain event under an earthquake of intensity at least, ν and the probability that a seismic demand D is larger than the capacity C of the event (Alli 2003) as follows

$$\lambda_{LS} = \nu \cdot P[D > C] \quad (1)$$

Mean annual frequency of exceeding a limit state is determined by splitting the above formula into seismic activity and structural parts. In the probabilistic seismic demand analysis method proposed by Cornell and Vamvatsikos (2002), the mean annual frequency of exceeding a limit state is computed as follows

$$\lambda_{LS} = \int_{IM=0}^{IM=\infty} F(IM^c | IM) \cdot \left| \frac{d\lambda_{IM}}{dIM} \right| dIM \quad (2)$$

In which dIM is the differential of the intensity measure. The absolute value is the gradient of the hazard with respect to IM , and $F(IM^c | IM)$ is the cumulative distribution function (CDF) of the occurrence of limit state capacity based on variable IM which is fragility curve. Since in this paper the intensity measure is the spectral acceleration at the first period with 5% damping, the spectral acceleration hazard is computed using power-law relationship, suggested by Luco and Cornell (1998)

$$\lambda_{S_a} = k_0 (S_a)^{-k} \quad (3)$$

In which parameters k_0 & k depend to seismic properties of the site.

By using numerical integration, the mean annual frequency of exceeding a limit state can be computed. From fragility curve, one can also compute the fragility probability in any given performance level for any given intensity measure level IM , without considering the seismic hazard, if the intensity measure is limited to the given level.

Demand capacity factor design format which is based on a technical framework for probabilistic performance-based design and assessment of structures proposed by Cornell and Jalayer (2003). Using Eq. (1) and total probability theorem (TPT), the mean annual frequency of exceeding a limit state can be computed by using Eq. (4)

$$\lambda_{LS} = \nu \cdot \sum_{all d} \sum_{all x} P[D > C | D = d] \cdot P[D = d | S_a = x] \cdot P[S_a = x] \quad (4)$$

In which ν is the average rate of occurrence of events with intensity measure higher than the

given minimum level, $P[D > C|D = d]$ is the conditional probability of having D larger than C given the demand is (limited to value) d , $P[S_a = x]$ is the probability of S_a being x , and $P[D = d|S_a = x]$ is the conditional probability of the demand being d given S_a is x .

In parallel, source of uncertainties can be categorized into “aleatory uncertainty” (as a result of inherent randomness) and “epistemic uncertainty” (as a result of knowledge limit). The former uncertainty can identify “natural variability”, which captures parameters such as time and parameters of future earthquakes and the variability in the amplitude and the phase of the acceleration history from one record to one other. The second type of uncertainty is based on lack and limitations of science and knowledge.

Using Eq. (4), adding certain (reasonable) hypothesis, e.g., the statistical independence of demand and capacity, after simplifications, one gets Eq. (5)

$$\lambda_{LS} = k_0 (S_a^{\eta_c})^{-k} \times e^{\frac{1}{2}\beta_{UH}^2} \times e^{\frac{1}{2b^2}(\beta_{RD}^2 + \beta_{UD}^2)} \times e^{\frac{1}{2b^2}(\beta_{RC}^2 + \beta_{UC}^2)} \quad (5)$$

In this equation, parameters k_0, k depend on seismic properties of the region, $S_a^{\eta_c}$ which can be computed using the interpolation of the incremental dynamical analysis mean curve and it is proportionate to the performance level. Coefficients a and b can be computed using the fitness function of the median curve. β_{UH} is the uncertainty parameter of spectral acceleration hazard and in this research it is assumed as 0.5 β_{RD} is the aleatory uncertainty parameter which is related to the demand variable (the maximum relative displacement between the floors). β_{UD} is the epistemic uncertainty which is related to the demand variable. To compute this parameter, Eq. (6) can be used

$$\beta_{UD} = \frac{\beta_{RD}}{\sqrt{n_{sample}}} \quad (6)$$

β_{RC} is the aleatory parameter which is related to the capacity and it is equal to

$$\beta_{RC} = \frac{\left(\ln \frac{S_a^{50\%}}{S_a^{16\%}} + \ln \frac{S_a^{84\%}}{S_a^{50\%}} \right)}{2} \quad (7)$$

β_{UC} is the epistemic parameter which is related to the capacity. To compute this parameter, Eq. (8) is used

$$\beta_{UC} = \frac{\beta_{RC}}{\sqrt{n_{sample}}} \quad (8)$$

In Eqs. (6)-(8), n_{sample} is the number of earthquake records in the dynamical analysis. $S_a^{16\%}$, $S_a^{50\%}$ and $S_a^{84\%}$ are the spectral acceleration of collapse prevention (CP) and immediate occupancy (IO) performance levels with various probabilities.

3. Design of studied frames

In this paper, performance level of steel buckling restrained braced frames with 4, 6, 8, 10, 12 and 14 stories and different bracing configuration including diagonal, split X, chevron (V and Inverted V) bracings have been studied using probabilistic method. In this regard total No. of 24 structures as mentioned above have been designed using IBC (2009) with the parameters S_{Ds} and

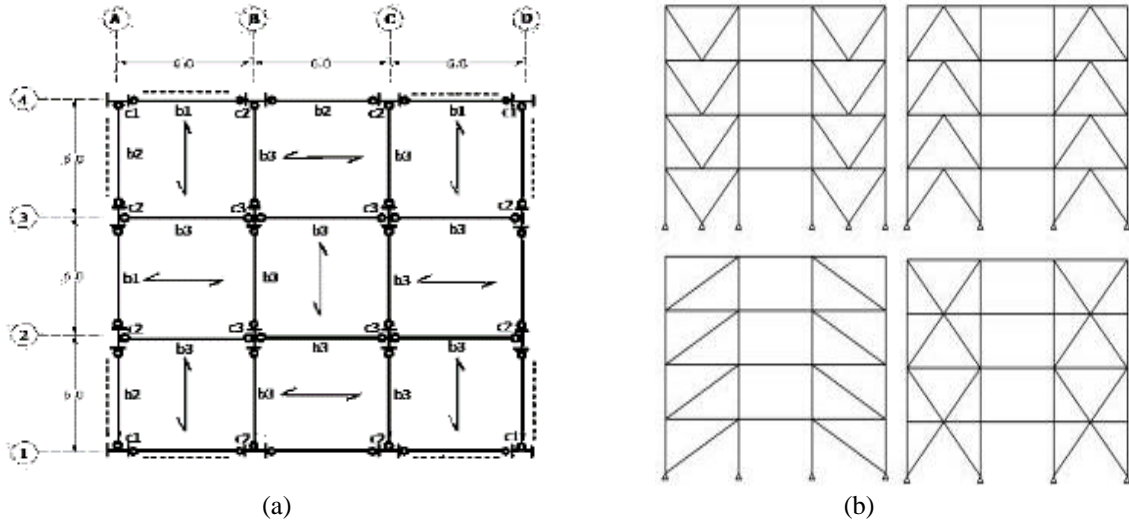


Fig. 2 (a), (b) Framing plan and vertical elevation of studied structures

Table 1 Cross sections of frame in row 4 of 4, 8 and 12-story structures with diagonal braces

	Number of Story	c1	c2	b1	b2	BRB (cm ²)
4-story	4	HE120B	HE160B	IPE330	IPE140	7
	3	HE120B	HE160B	IPE400	IPE220	11
	2	HE180B	HE240B	IPE400	IPE220	14
	1	HE180B	HE240B	IPE400	IPE220	15
8-story	8	HE120B	HE160B	IPE330	IPE140	6
	7	HE120B	HE160B	IPE400	IPE220	12
	6	HE180B	HE240B	IPE400	IPE220	16
	5	HE180B	HE240B	IPE400	IPE220	18
	4	HE260B	HE320B	IPE400	IPE220	21
	3	HE260B	HE320B	IPE400	IPE220	21
	2	HE300B	HE450B	IPE400	IPE220	21
12-story	1	HE300B	HE450B	IPE400	IPE220	24
	12	Box90×90×12.5	Box120×120×10	IPE330	IPE140	10
	11	Box90×90×12.5	Box120×120×10	IPE400	IPE220	16
	10	Box120×120×17.5	Box160×160×17.5	IPE400	IPE220	21
	9	Box120×120×17.5	Box160×160×17.5	IPE400	IPE220	23
	8	Box160×160×20	Box180×180×28	IPE400	IPE220	23
	7	Box160×160×20	Box180×180×28	IPE400	IPE220	24
	6	Box180×180×28	Box220×220×30	IPE400	IPE220	25
	5	Box180×180×28	Box220×220×30	IPE400	IPE220	26
	4	Box240×240×28	Box280×280×30	IPE400	IPE220	26
	3	Box240×240×28	Box280×280×30	IPE400	IPE220	27
	2	Box280×280×30	Box340×340×30	IPE400	IPE220	27
1	Box280×280×30	Box340×340×30	IPE400	IPE220	29	

S_{D1} equal to 1.1 and 0.65, respectively. Fig. 2(a), Fig. 2(b) show plan and elevation of 4-story structures. Span in both directions is 6 m and each story height is 3.2 m. The dead and live loads of 6.5 KN/m^2 and 2.0 KN/m^2 are considered respectively for design of structures, except roof live load which is considered as 1.5 KN/m^2 . Samples of frames section properties are shown in Table 1. Also, more details on assumption of structures design are presented in Appendix A.

4. Structural modeling using OpenSees software

Nonlinear dynamic analyses of the designed frames subjected to earthquake were performed using OpenSees software. (Mazzoni 2007) For simplicity, only frame in row 4 which represents behavior of whole structure subjected to earthquake has been analyzed. For the dynamic analysis, story masses were placed in the story levels considering rigid diaphragms action. Rayleigh damping matrix was used under the assumption of 5% damping for modes No. 1 & 2 and capability of last-committed state determination of stiffness matrix. In modeling of members in nonlinear range of deformation, Non-linear Beam Column Element based on displacement and fiber cross sections with uniaxial hysteretic material model were used. All the steel were modeled with a yield strength 235 MPa and strain hardening of 2%. (Fig. 3) For considering geometric stiffness of the frames, co-rotational transformation was used which takes into account large displacement effect accurately. Moreover, to consider possible in-plane buckling of columns caused by the axial loads, an initial mid-span imperfection of 1/1000 of member length was considered. The structural first period of each model is demonstrated in Table 2.

5. Incremental dynamic analysis

Incremental dynamic analysis of designed frames was performed subjected to sets of 13 ground motions as presented in Table 3. Ground motions were selected from recorded on soil type C as per IBC (2009). In this paper, first mode spectral acceleration and maximum interstory drift are considered as intensity measure (IM) and damage measure (DM) respectively.

Figs. 4(a)-(b) show diverse curves obtained by IDA for 14-story and 4-story diagonal braced frames as samples of other results. It can be seen the capacity and elastic stiffness of the taller frame is less than low rise one. 16%, 50% and 84% percentiles of IDA results of 4, 8 and 12-story frames with split X and diagonal bracing configuration are presented in Figs. 5-7 respectively. It can be seen that capacity of split X bracing type are more than diagonal bracing configuration. Diagonal configuration of ordinary bracing type are not recommended in common practice due to buckling of bracing and stiffness and strength deterioration in post buckling region, but this configuration inspite of lower capacity can be used as buckling restrained ones. As a sample, median IDA curve of chevron (Inverted V and V) type bracing for different No. of stories are compared in Figs. 8 and 9 respectively. It can be seen that the behavior of both of chevron type (V and inverted V) is more or less the same. Figs. 10-12 show median curves obtained by incremental dynamic analysis for 4, 8 and 12-story frames with different bracing configuration. It can be shown that stiffness of diagonal type is less than the others. Meanwhile, the capacity of chevron and split X types are in the same range and more than diagonal type for low and middle rise (4 and 8-story) frames. In 12-story frame, due to satisfying frames drift during design stage, stiffness and strength of all of designed frames are more and less the same. The elastic stiffness of the models

drops as the height of the frame increases.

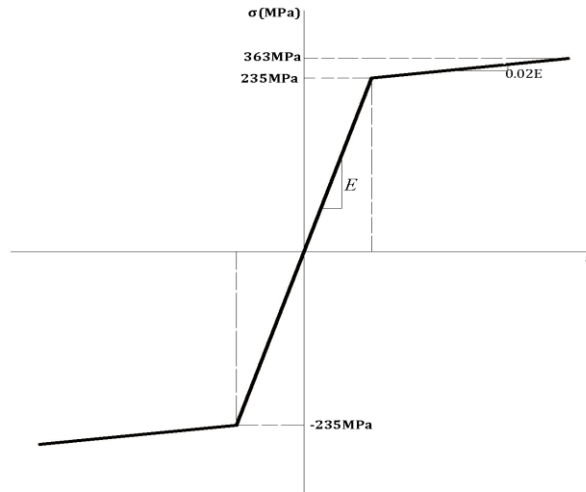


Fig. 3 uniaxial hysteretic material for buckling restrained braces

Table 2 Structural first period

No. Story	BRB configuration	$T_1(sec)$
4-story	Diagonal	0.8998
	Chevron (V)	0.7640
	Inverted chevron (Λ)	0.6679
	Spilt (X)	0.7653
6-story	Diagonal	1.2023
	Chevron (V)	1.0707
	Inverted chevron (Λ)	0.9698
	Spilt (X)	1.0404
8-story	Diagonal	1.5313
	Chevron (V)	1.4048
	Inverted chevron (Λ)	1.2586
	Spilt (X)	1.3523
10-story	Diagonal	1.8374
	Chevron (V)	1.7397
	Inverted chevron (Λ)	1.5905
	Spilt (X)	1.6789
12-story	Diagonal	2.1490
	Chevron (V)	2.0401
	Inverted chevron (Λ)	1.9257
	Spilt (X)	1.9956
14-story	Diagonal	2.4063
	Chevron (V)	2.3048
	Inverted chevron (Λ)	2.2205
	Spilt (X)	2.2930

Table 3 Ground motion records

No	Earthquake Location	Year	Station	time (sec)	R (Km)	M	PGA (g)
1	Chi-Chi, Taiwan	1999	TCU070	90	19.1	7.6	0.255
2	Victoria, Mexico	1980	6604 Cerro Prieto	24.45	34.8	6.1	0.587
3	Whittier Narrows	1987	116th St School LA -14403	40	22.5	6	0.396
4	Northridge	1994	24605 LA - Univ. Hospital	40	34.6	6.7	0.493
5	Kocaeli, Turkey	1999	Mecidiyekoy	44	62.3	7.4	0.068
6	Northridge	1994	24607 Lake Hughes #12A	40	22.8	6.7	0.257
7	Northridge	1994	90021 LA-N Westmoreland	30	29	6.7	0.401
8	Chi-Chi, Taiwan	1999	TCU045	90	24.06	7.6	0.512
9	Loma Prieta	1989	57504 Coyote Lake Dam (Downst) LOMAP/CLD195	39.95	22.3	6.9	0.16
10	Northridge	1994	90014 Beverly Hills - 12520 Mulhol(NORTHR/MU2035)	23.98	20.8	6.7	0.617
11	Imperial Valley	1979	286 Superstition Mtn Camera	28.28	26	6.5	0.195
12	N. Palm Springs	1986	13123 Riverside Airport(PALMSPR/RIV270)	25	71.1	6	0.04
13	Morgan Hill	1984	57007 Corralitos	36	22.7	6.2	0.109

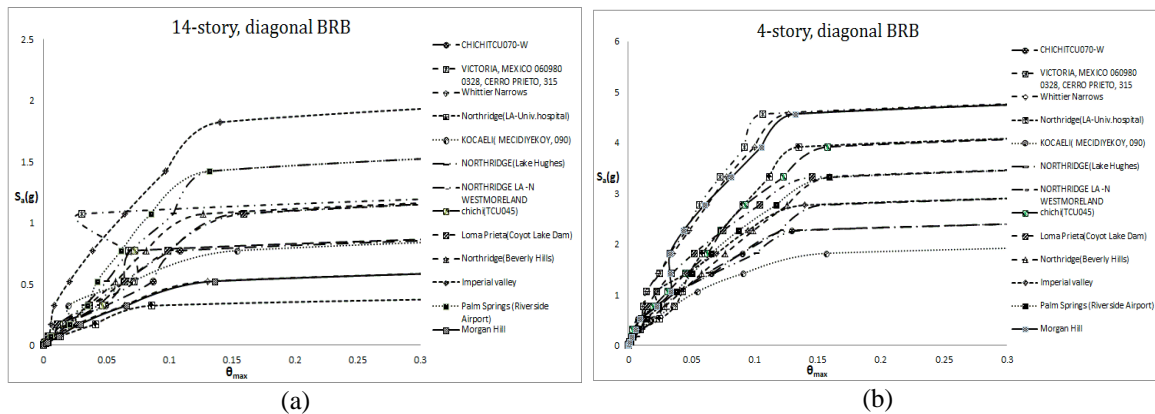


Fig. 4 non-linear incremental dynamic analyses of diagonal braces (a) 14-story (b) 4-story

In order to obtain seismic performance of the frames, two performance levels, immediate occupancy (IO) and collapse prevention (CP), were chosen. Based on FEMA 350, the story drift for IO and CP performance levels were set to 2% and 10% respectively. For CP performance level, another criterion was also checked in which slope of IDA curve was considered as 20% of the primary elastic slope. FEMA 350 (2000)

The values of S_a for both IO and the CP performance levels in 16%, 50% and 84% percentiles is presented in Fig. 13. It can be seen that as the height of the frames increases, the “capacity of structure” decreases. Moreover, in frames with small and medium height (4, 6, 8 and 10-story models), the capacity of models with inverted chevron braces and chevron V braces are more than the capacity of models with spilt X braces and diagonal braces for all of percentiles.

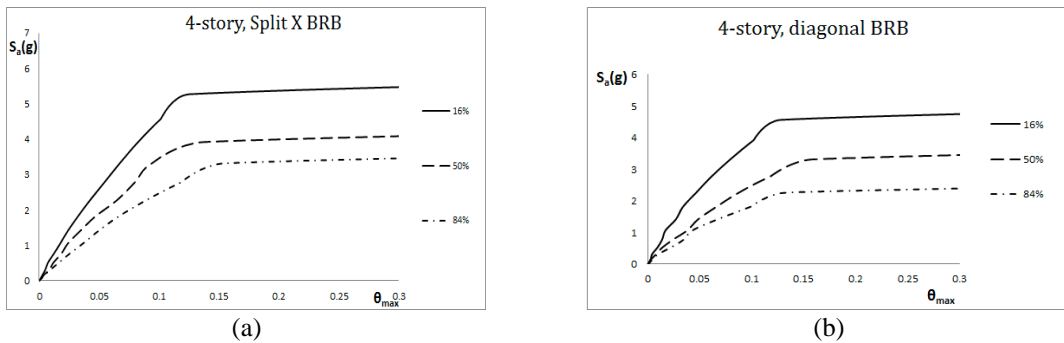


Fig. 5 statistical percentiles 16%, 50% and 84% of 4-story models (a) split X brace (b) diagonal brace

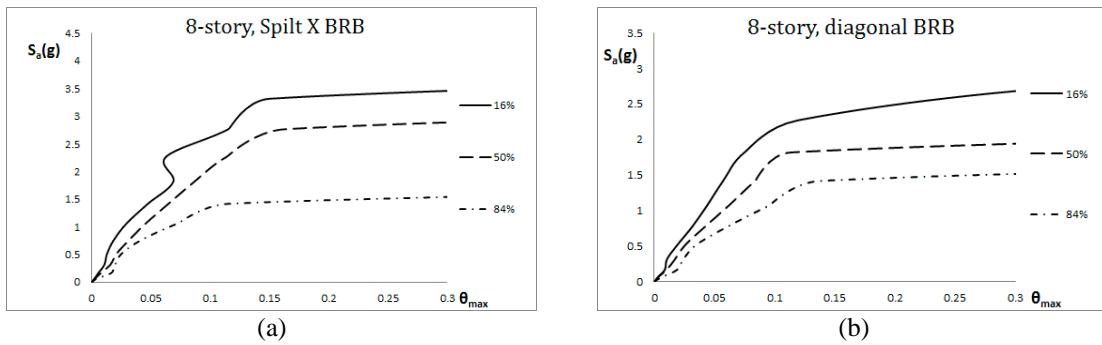


Fig. 6 statistical percentiles 16%, 50% and 84% of 8-story models (a) split X brace (b) diagonal brace

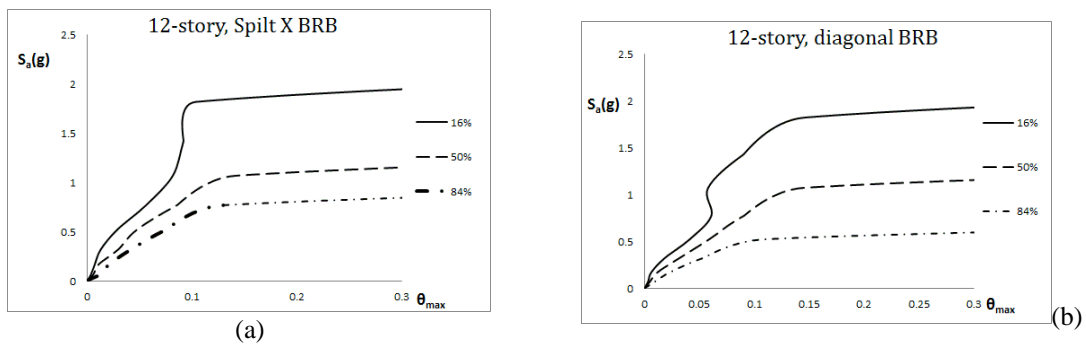


Fig. 7 statistical percentiles 16%, 50% and 84% of 12-story models (a) split X brace (b) diagonal brace

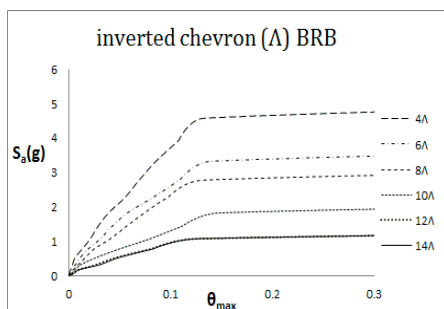


Fig. 8 median curves for inverted chevron braces

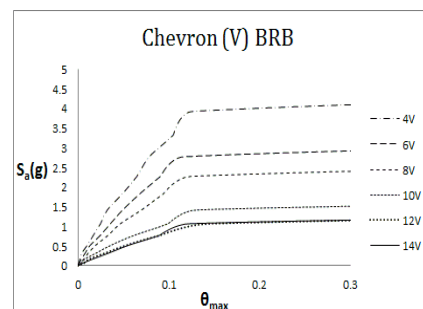


Fig. 9 median curves for chevron V braces

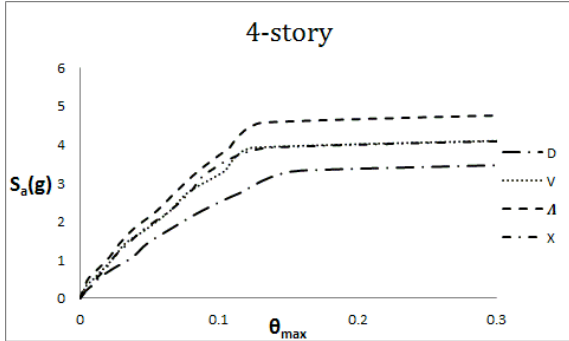


Fig. 10 median curves for 4-story models

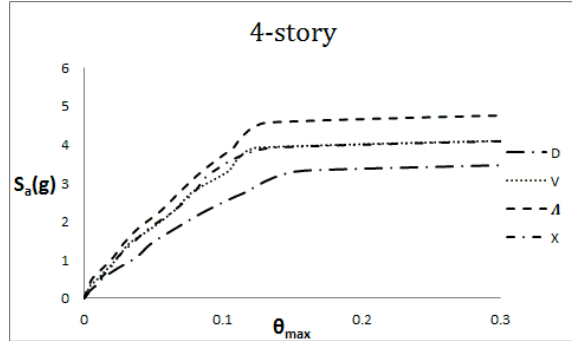


Fig. 11 median curves for 8-story models

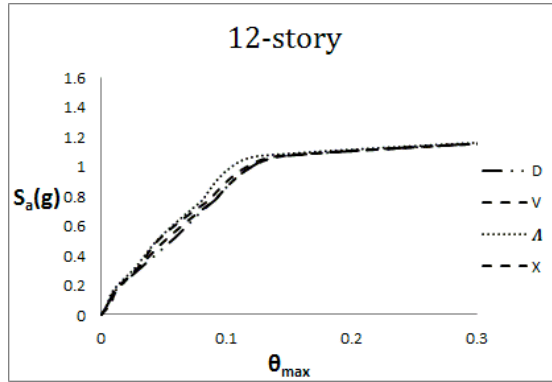


Fig. 12 median curves for 12-story models

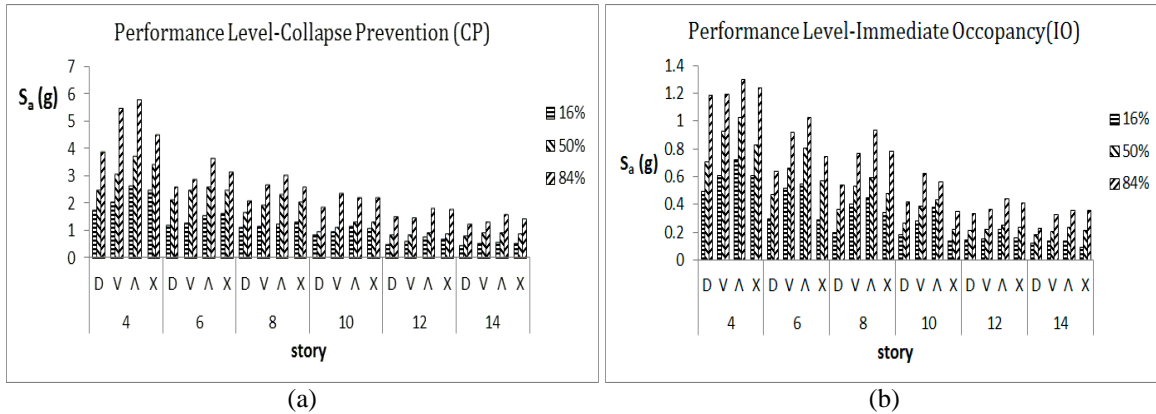


Fig. 13 values of S_a in various percentiles (a) CP performance level (b) IO performance level

6. Computing mean annual frequency of exceeding limit states

In order to compute the seismic parameters k and k_0 , the seismic hazard analysis of the region near Tehran with latitude 36.37° and longitude 52.33° was used. (Research Report 2011) Table 4 shows parameters k and k_0 for different period for the selected location.

Table 4 seismic parameters k, k_0

$T_1(sec)$	0.775	1.071	1.387	1.712	2.028	2.306
k_0	1.90E-03	7.18E-04	2.60E-04	1.23E-04	6.76E-05	7.00E-05
k	2.26387	2.29019	2.28809	2.24682	2.37415	2.04296

6.1 Fragility curve

Figs. 14-17 show fragility curves for different types of bracing configuration. In each of above figures, fragility curves for performance levels of CP and IO were compared for different frames. Figs. 18-23 compare fragility curve of frames with various configurations of braces and fixed height for both CP and IO levels. According to Figs. 14-17 fragility probability is increased as the number of stories is increased. Also, these curves indicate that fragility probability in 12 and 14-story frames have no major difference. It should be pointed that fragility probability increase rate is decreased by height increase. It can also be observed from Figs. 18-20 that in collapse prevention (CP) level, prevailingly diagonal buckling restrained brace has the most fragility probability and inverted chevron brace has the least probability. Furthermore chevron V brace has more fragility probability than split X brace. Figs. 21-23 denote that fragility probability of inverted chevron brace in immediate occupancy (IO) level is less than other buckling restrained braces. Furthermore, diagonal brace has the most fragility probability. Besides, split X brace usually have more fragility probability than chevron V brace.

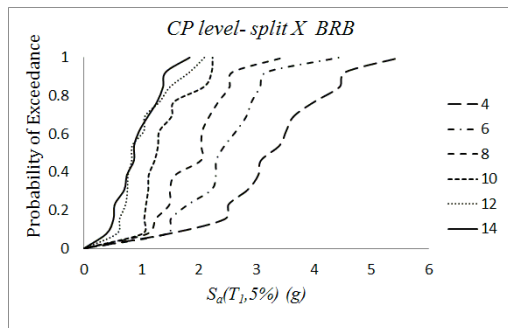


Fig. 14 Fragility curves of split X BRB, CP level

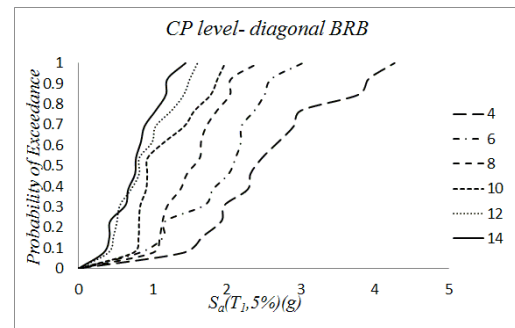


Fig. 15 Fragility curves of diagonal BRB, CP level

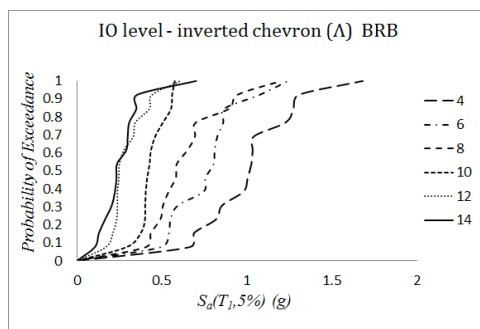


Fig. 16 Fragility curves for inverted chevron, IO level

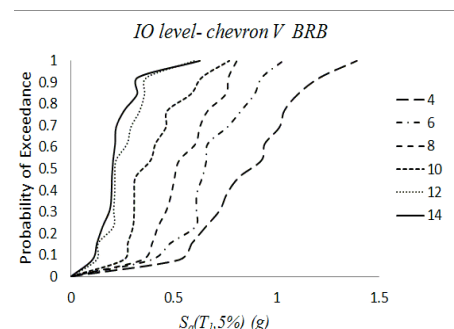


Fig. 17 Fragility curves of chevron V, IO level

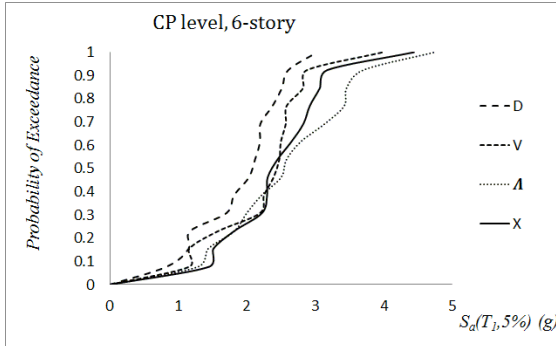


Fig. 18 Fragility curves of 6-story models, CP level

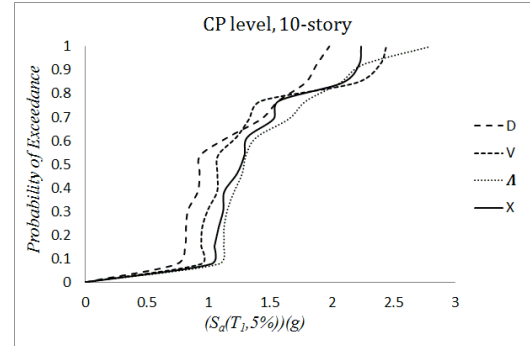


Fig. 19 Fragility curves of 10-story models, CP level

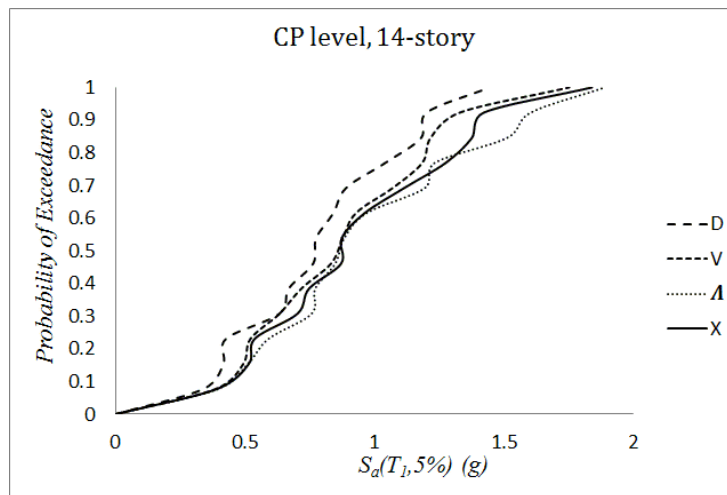


Fig. 20 Fragility curves of 14-story models, CP level

6.2 Computing of mean annual frequency of exceeding limit states with probabilistic seismic demand analysis method (PSDA):

By using probabilistic seismic demand analysis method, mean annual frequency was calculated through numerical integration of Eq. (2). (Figs. 24(a)-(b))

Fig. 24(a) shows in Immediate Occupancy level inverted chevron and chevron V buckling restrained braces have better performance than diagonal and split X buckling restrained braces. Moreover in this performance level inverted chevron buckling restrained braces have better performance than chevron V buckling restrained braces. Also, diagonal buckling restrained braces has the weakest performance in 4, 8 and 12 stories models. Moreover, split X buckling restrained braces in 6, 10 and 14 stories models have the most inappropriate performance. According to Fig. 24(b), in collapse prevention level, split X and inverted chevron buckling restrained braces have more appropriate performance than diagonal and chevron V buckling restrained braces. Furthermore, split X buckling restrained brace in 4, 6 and 8-story models have better performance than inverted chevron buckling restrained braces. Also, inverted chevron buckling restrained braces in 10, 12, 14-story models, have better performance than split X buckling restrained braces.

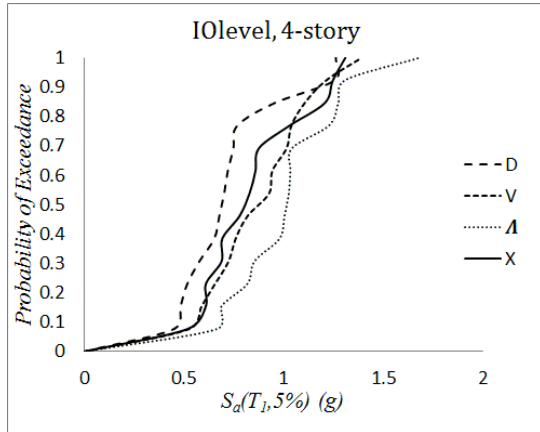


Fig. 21 Fragility curves of 4-story models, IO level

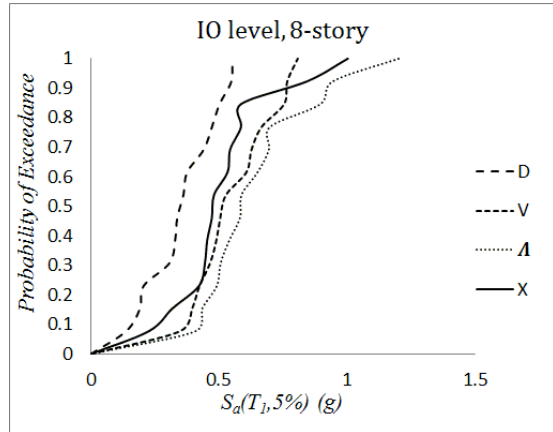


Fig. 22 Fragility curves of 8-story models, IO level

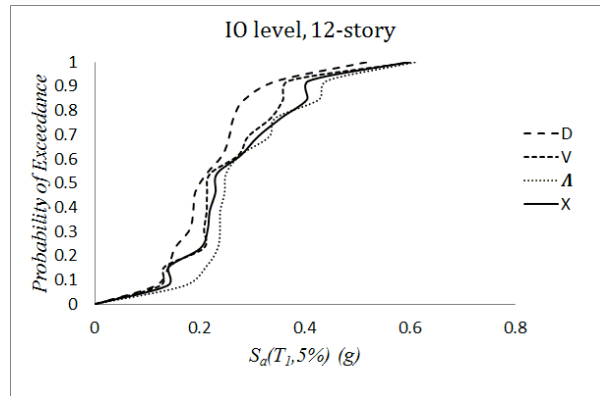
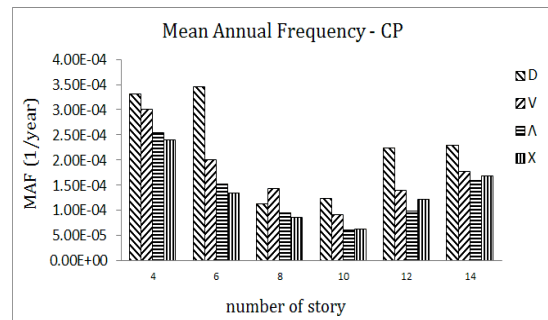
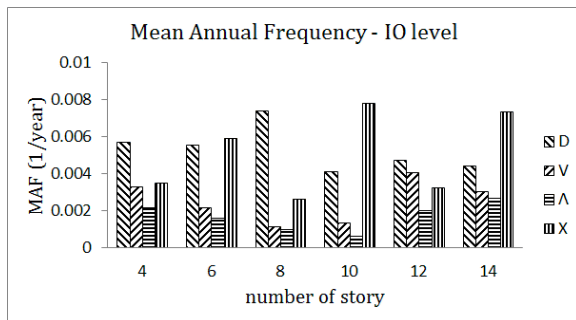


Fig. 23 Fragility curves for 12-story models, IO level



(a)

(b)

Fig. 24 MAF, (a) IO level (b) CP level

6.3 Displacement-based strategy solution in capacity-demand factor design (DCFD) form

In this paper, each S_a related to each performance level, was also calculated by linear interpolation from median curves resulted of incremental dynamic analysis. (see Figs. 25(a)-(b)).

With a regression function e.g., $\theta_{max} = a(S_a^{50\%})^b$, a and b parameters in median curves obtained by incremental dynamic analysis was also calculated. (see Fig. 26)

To compute β_{RD} , at first the distance between CP performance level and IO performance level on median curve are specified from 16% and 84% curves. Then Eq. (6) was used for β_{UD} Calculation (see Figs. 27-28). β_{RC} (see Fig. 29) was also calculated by using Eq. (7) and diagrams of S_a associated with different occurrence probability of CP and IO (consider Figs. 12(a)-(b)). Moreover β_{UC} (see Fig. 30) was calculated using Eq. (8). Using Eq. (5) evaluated mean annual frequency are shown in Figs. 31(a)-(b). Considering Fig. 31(a), inverted chevron braces

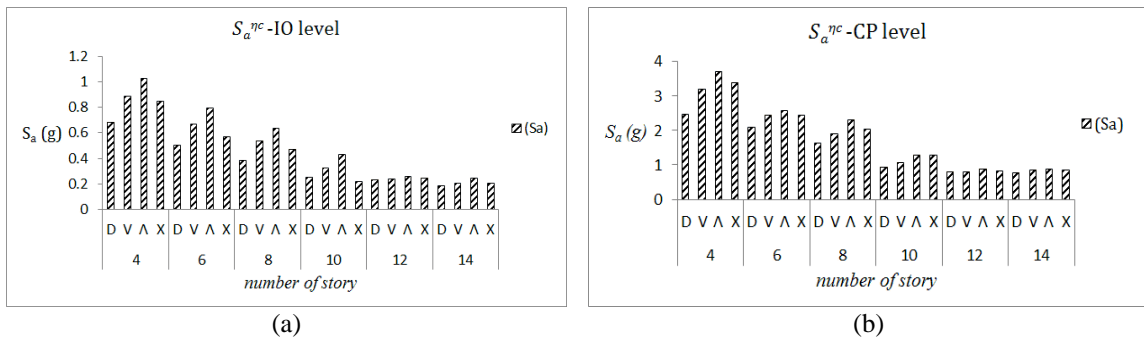


Fig. 25 $S_a^{\eta_c}$ (a) IO level (b) CP level

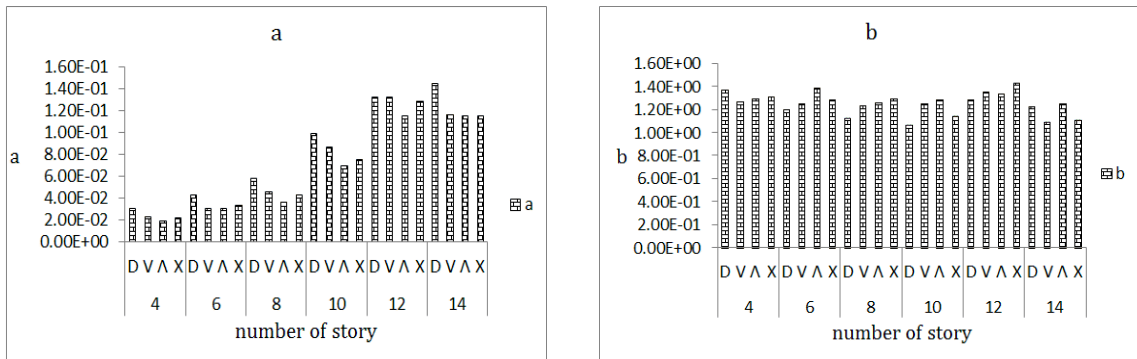


Fig. 26 a, b parameters

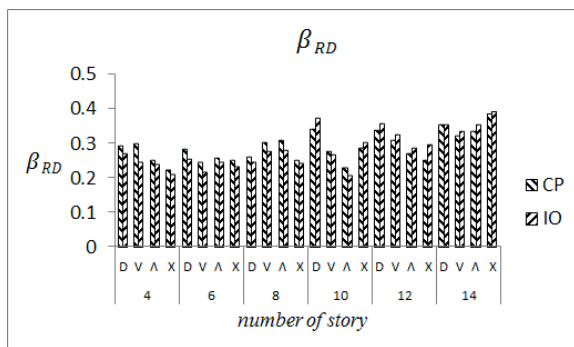


Fig. 27 β_{RD}

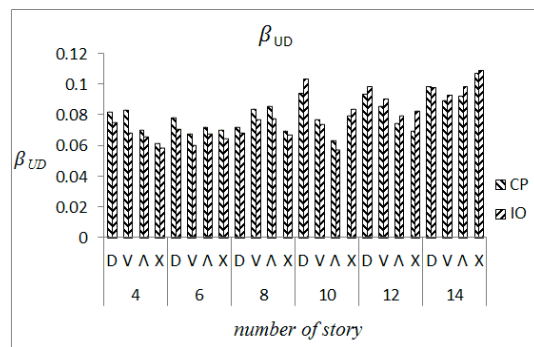


Fig. 28 β_{UD}

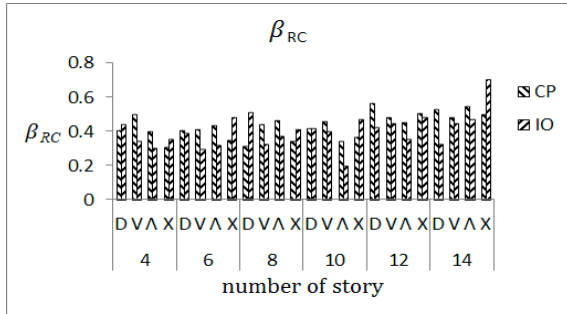


Fig. 29 β_{RC}

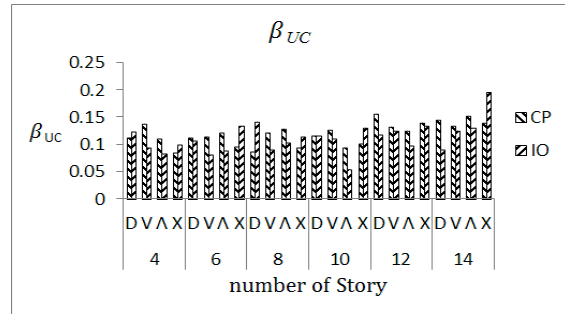
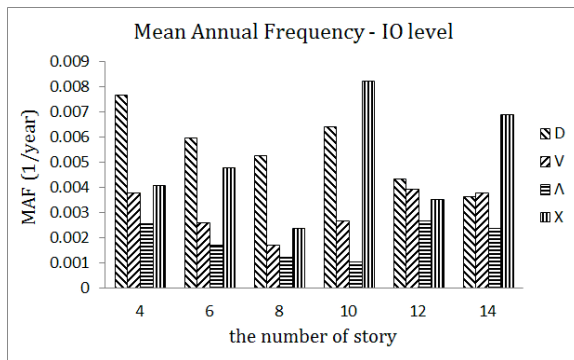
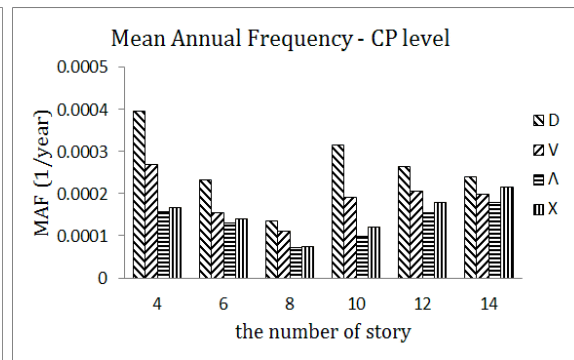


Fig. 30 β_{UC}



(a)



(b)

Fig. 31 mean annual frequency (a) IO level, (b) CP level

have better performance compared to other type of buckling restrained braces. Moreover in 4, 6, 8 and 12 stories models diagonal has weakest performance. Also, after inverted chevron, chevron V has proper performance. Considering Fig. 31(b), in all supposed models, inverted chevron (Λ) has the best performance. Furthermore diagonal buckling restrained braces have the weakest performance. In addition, the mean annual frequency of exceeding collapse prevention level in split X buckling restrained braces is less than chevron V buckling restrained braces.

6.4 Comparison of PSDA and DCFD methods results

Considering the results of both methods, it can be seen that PSDA results are different from DCFD results. This difference indicates the effect of various uncertainties including hazard analysis uncertainties, demand and capacity uncertainty in mean annual frequency assessment. (see Figs. 31(a)-(b))

7. Conclusions

In this paper, probabilistic seismic evaluation of buckling restrained braced frames has been implemented by DCFD and PSDA methods for different BRB configurations as well as diverse number of stories so that fragility curves and mean annual frequency of exceeding immediate

occupancy (IO) and collapse prevention (CP) limit states can be estimated by results that has been obtained by incremental dynamic analysis. Hence, 4 BRB configurations (chevron, inverted chevron, diagonal and spilt X) and 4, 6, 8, 10, 12 and 14-story frames were considered to assess their impact on probabilistic quantities. Furthermore, uncertainties effect was also probed. Following results can be concluded:

- By increasing the height of the studied braced frames, the values of first mode spectral acceleration of median curves decreases significantly.
- For most of the frames, inverted chevron buckling restrained braces have the most S_a capacity. Afterwards, split X buckling restrained braces, chevron V buckling restrained braces and diagonal buckling restrained braces respectively, have the most S_a capacity.
- With frame height increase, fragility probability in performance levels including Immediate Occupancy' and Collapse Prevention increases. This is due to the damaging nature of earthquakes in higher structures.
- In general, in braced frames with buckling restrained braces with the same height and without considering the seismic hazard, the diagonal buckling restrained braces in collapse prevention and immediate occupancy limit states, have the highest fragility probability. Moreover, the inverted chevron braces have the lowest fragility probability due to high energy absorption capacity.
- In general, in same-height models in collapse prevention limit state, inverted chevron and spilt X buckling restrained braced frames have a better performance compared to V and diagonal frames. In immediate occupancy limit state inverted chevron buckling restrained braces have the best performance compared to other buckling restrained braces.
- The results from PSDA method is different from solution based on displacement in DCFD method. This is due to ignoring some uncertainties such as the uncertainty in hazard analysis, uncertainty in estimating the median of demand and capacity and also error in numerical integration. So it can be concluded “uncertainties” are very effective in mean annual frequency of exceeding limit states.
- With frame height increase, fragility probability in performance levels including Immediate Occupancy' and Collapse Prevention increases. This is due to the damaging nature of earthquakes in higher structures.
- In general, in braced frames with buckling restrained braces with the same height and without considering the seismic hazard, the diagonal buckling restrained braces in collapse prevention and immediate occupancy limit states, have the highest fragility probability. Moreover, the inverted chevron braces have the lowest fragility probability due to high energy absorption capacity.

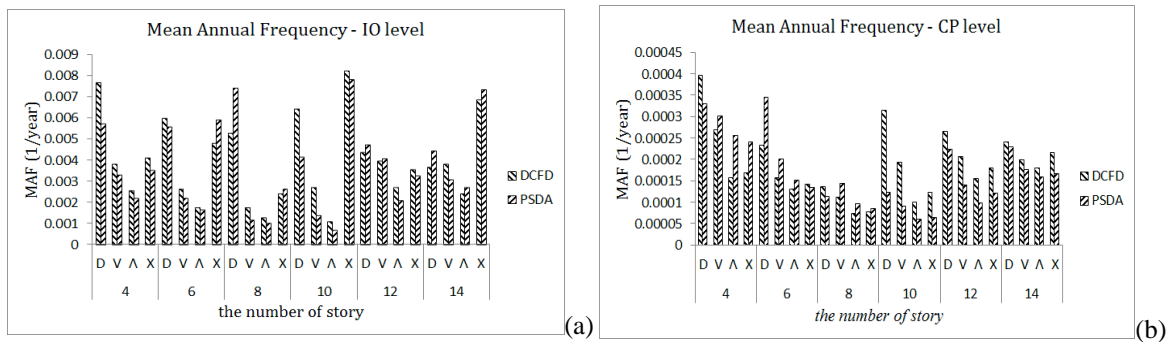


Fig. 32 results of mean annual frequency of exceeding by two methods (a) IO level (b) CP level

- In general, in same-height models in collapse prevention limit state, inverted chevron and split X buckling restrained braced frames have a better performance compared to V and diagonal frames. In immediate occupancy limit state inverted chevron buckling restrained braces have the best performance compared to other buckling restrained braces.
- The results from PSDA method is different from solution based on displacement in DCFD method. This is due to ignoring some uncertainties such as the uncertainty in hazard analysis, uncertainty in estimating the median of demand and capacity and also error in numerical integration. So it can be concluded “uncertainties” are very effective in mean annual frequency of exceeding limit states.

References

- Asgarian, B. and Shokrgozar, H.R. (2009), “BRBF response modification factor”, *J. Constr. Steel Res.*, **65**(2), 290-298.
- Bozorgnia, Y., Bertero, V.V., Uang, C.M. and Nakashima, M. (2003), *Earthquake Engineering From Engineering Seismology To Performance-based Engineering*, CRC press, New York, USA.
- Clark, P., Aiken, I., Tajirian, F.F., Kasai, K., Ko, E. and Kimura, I. (1999), “Design procedures for buildings incorporating hysteretic damping devices”, *Design Procedures for Buildings Incorporating Hysteretic Damping Devices*, **1**(1), 1-21.
- FEMA 350 (2000), *Recommended seismic design criteria for new steel moment-frame buildings*, SAC Joint Venture, Federal Emergency Management Agency, Washington, DC., Report No. FEMA-350.
- Güneyisi, E.M. (2012), “Seismic reliability of steel moment resisting framed buildings retrofitted with buckling restrained braces”, *Earthq. Eng. Struct. Dyn.*, **41**(5), 853-874.
- Hoveidae, N. and Rafezy, B. (2012), “Overall buckling behavior of all-steel buckling restrained braces”, *J. Constr. Steel Res.*, **79**, 151-158.
- International Building Code (2009), International Building Council, Inc.
- Iranian building codes and standards (2005), *Iranian code of practice for seismic resistance design of buildings, Standard no. 2800-05 (3rd edition)*, Tehran.
- Iranian National Building Code (2008), 10th part, steel structure design. *Tehran (Iran): Ministry of Housing and Urban Development*.
- Jalayer, F. and Cornell, C.A. (2003), “A technical framework for probability-based demand and capacity factor (DCFD) seismic formats”, RMS.
- Ju, Y.K., Kim, M.H., Kim, J. and Kim, S.D. (2009), “Component tests of buckling-restrained braces with unconstrained length”, *Eng. Struct.*, **31**(2), 507-516.
- Kumar, G.R., Kumar, S.S. and Kalyanaraman, V. (2007), “Behaviour of frames with Non-Buckling bracings under earthquake loading”, *J. Constr. Steel Res.*, **63**(2), 254-262.
- Lin, K.C., Lin, C.C.J., Chen, J.Y. and Chang, H.Y. (2010), “Seismic reliability of steel framed buildings”, *Struct. Saf.*, **32**(3), 174-182.
- Luco, N. and Cornell, C.A., (1998), “Seismic drift demands for two SMRF structures with brittle connections”, *Structural Engineering World Wide 1998*, Elsevier Science Ltd., Oxford, England, Paper T158-3.
- Mazzoni, S., McKenna, F., Scott, M.H., Fenves, G.L. and Jeremic, B. (2007), “OpenSees Command Language Manual”.
- Park, Junhee, Lee, Junho and Kim, Jinkoo (2012), “Cyclic test of buckling restrained braces composed of square steel rods and steel tube”, *Steel Compos. Struct.*, **13**(5), 423-436.
- Rai, D.C. and Goel, S.C. (2003), “Seismic evaluation and upgrading of chevron braced frames”, *J. Constr. Steel Res.*, **59**(8), 971-994.
- Research Report (2011), “Probabilistic Seismic hazard analysis phase I - greater Tehran regions final report”.

<http://iranhazard.mporg.ir/>

Sabelli, R., Mahin, S. and Chang, C. (2003), "Seismic demands on steel braced frame buildings with buckling-restrained braces", *J. Eng. Struct.*, **25**(5), 655-666.

Tsai, Keh-Chyuan, Weng, Yuan-Tao, Lin, Sheng-Lin and Goel, Subhash (2004), "Pseudo-dynamic test of a full-scale CFT/BRB frame, part 1- performance based specimen design", *13th World Conference on Earthquake Engineering*, Vancouver, Canada.

Vamvatsikos, D. and Cornell, C.A. (2002), "Seismic performance, capacity and reliability of structures as seen through incremental dynamic analysis", Ph.D. Dissertation, Stanford university, Stanford, USA.

CC

Appendix. A Design details of building

According to the Iranian Seismic Code No. 2800 (Standard no. 2800 (3rd edition) 2005), Tehran is located in the very high seismic zone with a design earthquake acceleration of 0.35 g. (See Table 4)

The design base shear is computed by the following equation

$$V = CW \rightarrow C = \frac{ABI}{R} \tag{9}$$

Where V is base shear of structure, C is seismic coefficient and W is the equivalent weight of the structure calculated in accordance with Eq. (A2)

$$W = Dead\ Load + \beta \times LiveLoad \quad 0 < \beta < 1 \tag{10}$$

For the occupancy being considered β is equal to 0.2.

$A \cdot B$ is the spectral acceleration of the design which is based on the gravitational acceleration and it depends on the fundamental period, site's soil type and site's seismicity. I and R are importance factor and behavioral factor, respectively. In this study, the site's soil type to II, (average shear wave velocity to a depth of 30 m would be 360–750 m/s) $I=1$ and $R=10$ was considered. For design purposes, the method of allowable stress is used. And the braces are designed to withstand 100% of the lateral forces. It is worth mentioning that all the connections of beams and columns in both ends were considered hinge. To be certain about the resistance of columns against the transmitted axial force, the following load combinations were used in design. Iranian National Building Code, part 10 (2008)

a) Axial compression according to: $0.75(P_D + P_L + 2P_E) \leq F_a A \tag{11}$

b) Axial tension according to: $0.75(P_D + 2P_E) \leq 0.6F_y A \tag{12}$

In the above expressions, P_D , P_L and P_E are the axial forces induced by the dead load, the live load and the earthquake load, respectively. Based on standard no. 2800, 3rd edition, the real-relative displacement of design in each story should not be larger than the following values. (In these equations h is the height of each story of the building.)

a) Fundamental period of less than 0.7 seconds: $\bar{\Delta}_M < 0.025h \tag{13}$

b) Fundamental period of more than 0.7 seconds: $\bar{\Delta}_M < 0.02h \tag{14}$

Table 4 Earthquake acceleration for different seismic regions (Standard no. 2800 (3rd edition) 2005)

Zone	Seismic Hazard	Earthquake Acceleration (g)
1	Very high	0.35
2	High	0.30
3	Medium	0.25
4	Low	0.2